

A Supplementary File for  
“An Analysis of Control Parameters of MOEA/D  
Under Two Different Optimization Scenarios”

Ryoji Tanabe, Hisao Ishibuchi\*

*Shenzhen Key Laboratory of Computational Intelligence, Department of Computer Science  
and Engineering, Southern University of Science and Technology, Shenzhen, 518055, China*

---

**Abstract**

This is a supplementary file for “An Analysis of Control Parameters of MOEA/D  
Under Two Different Optimization Scenarios”.

---

---

\*Corresponding author

*Email addresses:* `rt.ryoji.tanabe@gmail.com` (Ryoji Tanabe), `hisao@sustc.edu.cn`  
(Hisao Ishibuchi)

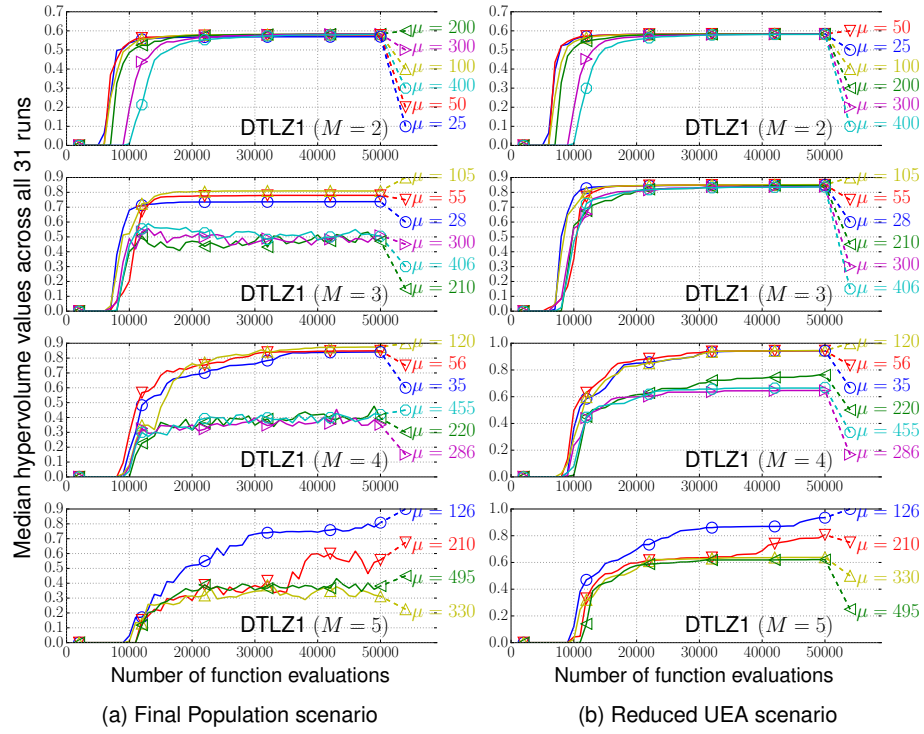


Figure S.1: Performance of MOEA/D with various  $\mu$  settings on the DTLZ1 problem with  $M \in \{2, 3, 4, 5\}$ . The horizontal and vertical axes represent the number of function evaluations and the HV values, respectively.

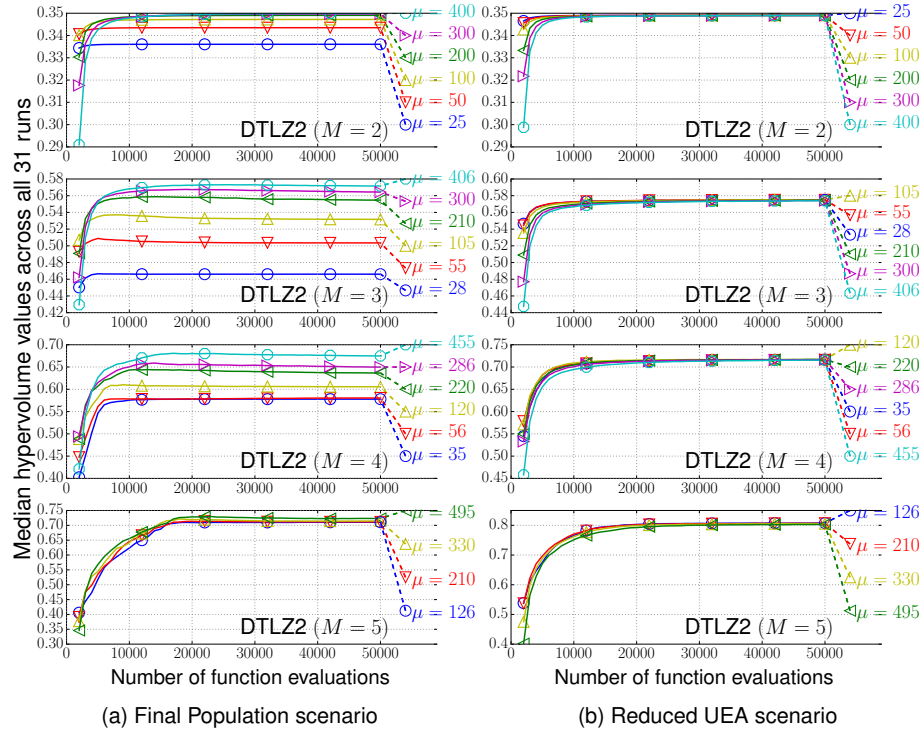


Figure S.2: Performance of MOEA/D with various  $\mu$  settings on the DTLZ2 problem with  $M \in \{2, 3, 4, 5\}$ . The horizontal and vertical axes represent the number of function evaluations and the HV values, respectively.

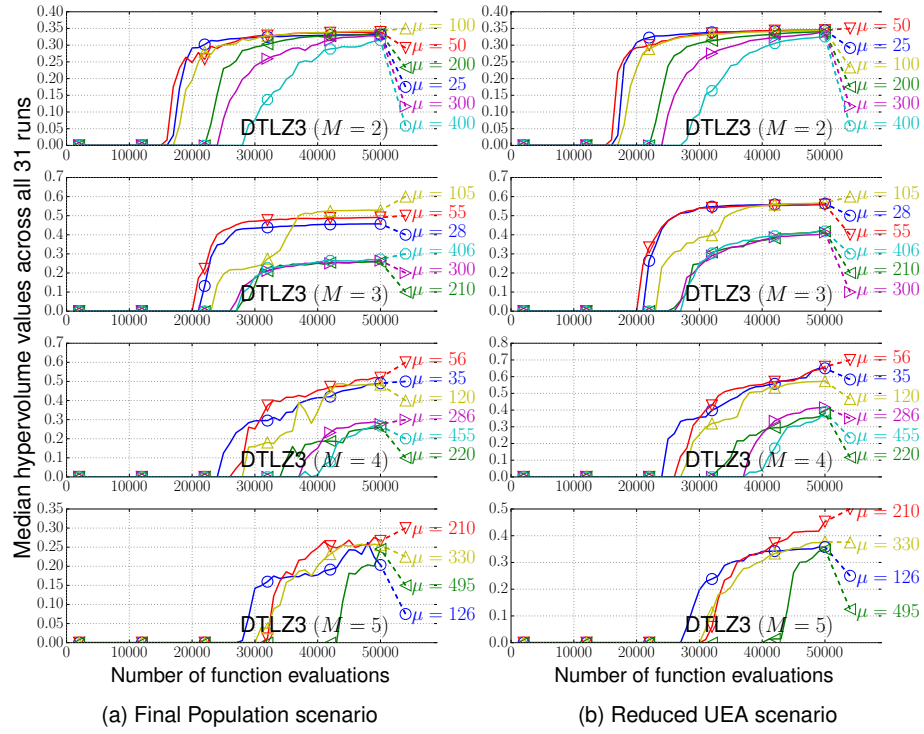


Figure S.3: Performance of MOEA/D with various  $\mu$  settings on the DTLZ3 problem with  $M \in \{2, 3, 4, 5\}$ . The horizontal and vertical axes represent the number of function evaluations and the HV values, respectively.

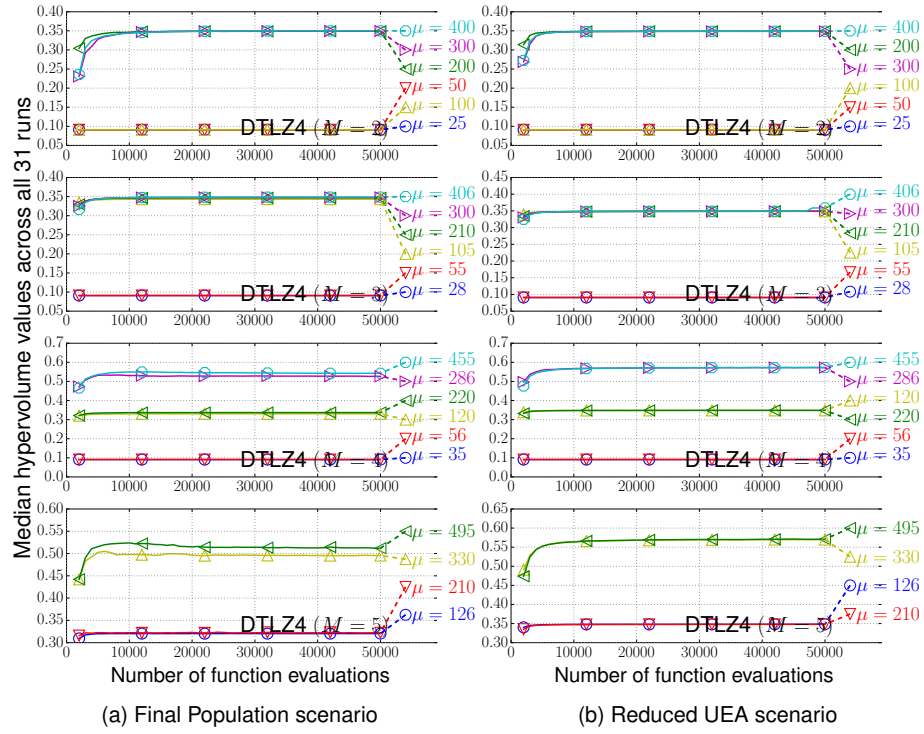


Figure S.4: Performance of MOEA/D with various  $\mu$  settings on the DTLZ4 problem with  $M \in \{2, 3, 4, 5\}$ . The horizontal and vertical axes represent the number of function evaluations and the HV values, respectively.

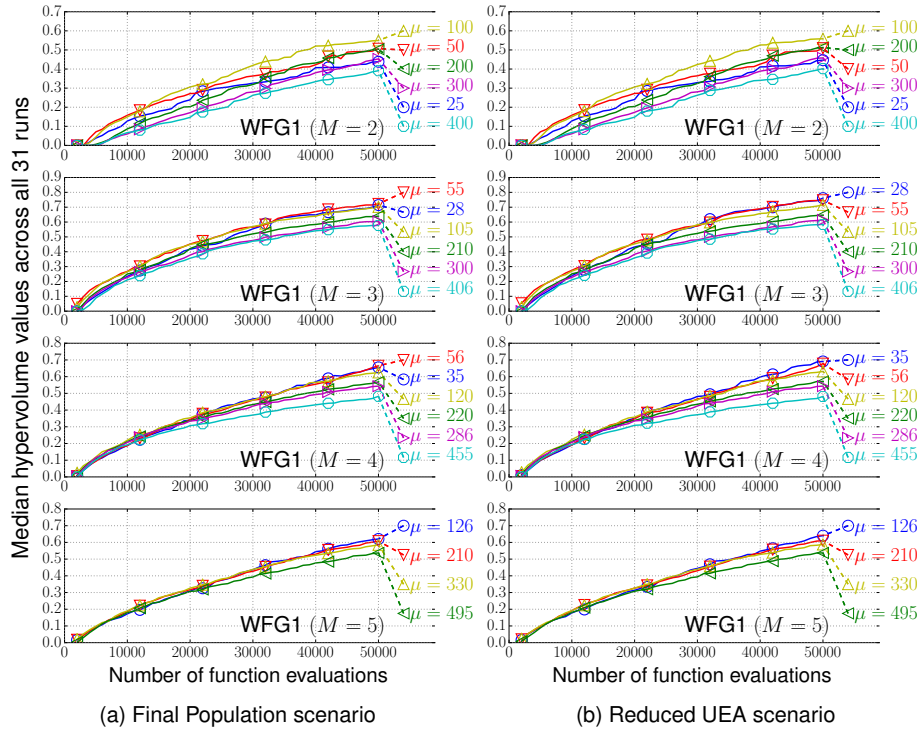


Figure S.5: Performance of MOEA/D with various  $\mu$  settings on the WFG1 problem with  $M \in \{2, 3, 4, 5\}$ . The horizontal and vertical axes represent the number of function evaluations and the HV values, respectively.

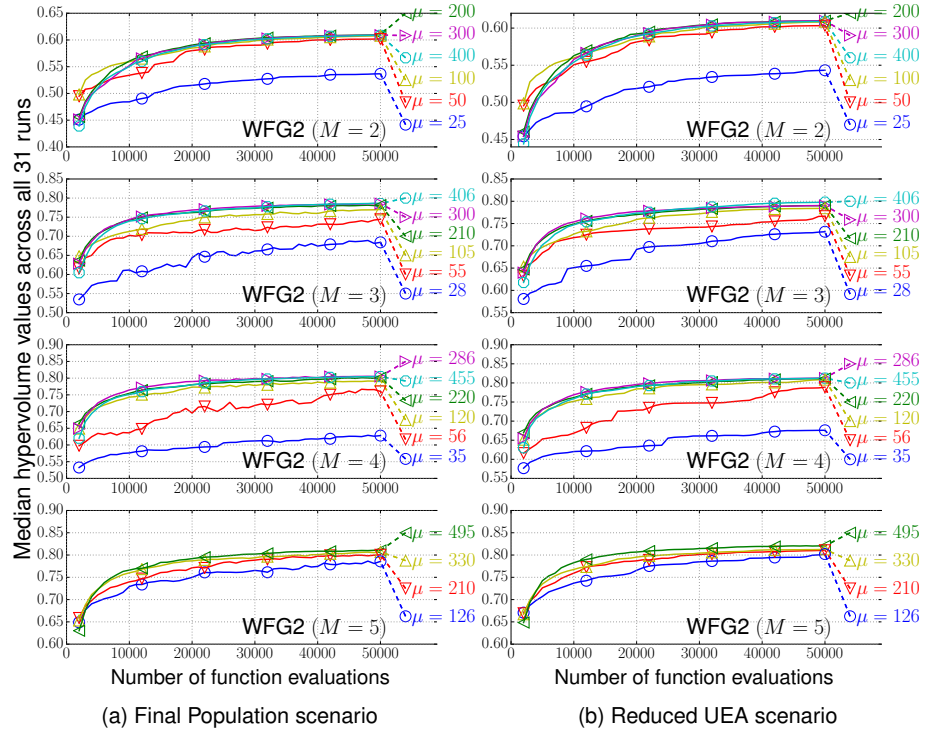


Figure S.6: Performance of MOEA/D with various  $\mu$  settings on the WFG2 problem with  $M \in \{2, 3, 4, 5\}$ . The horizontal and vertical axes represent the number of function evaluations and the HV values, respectively.

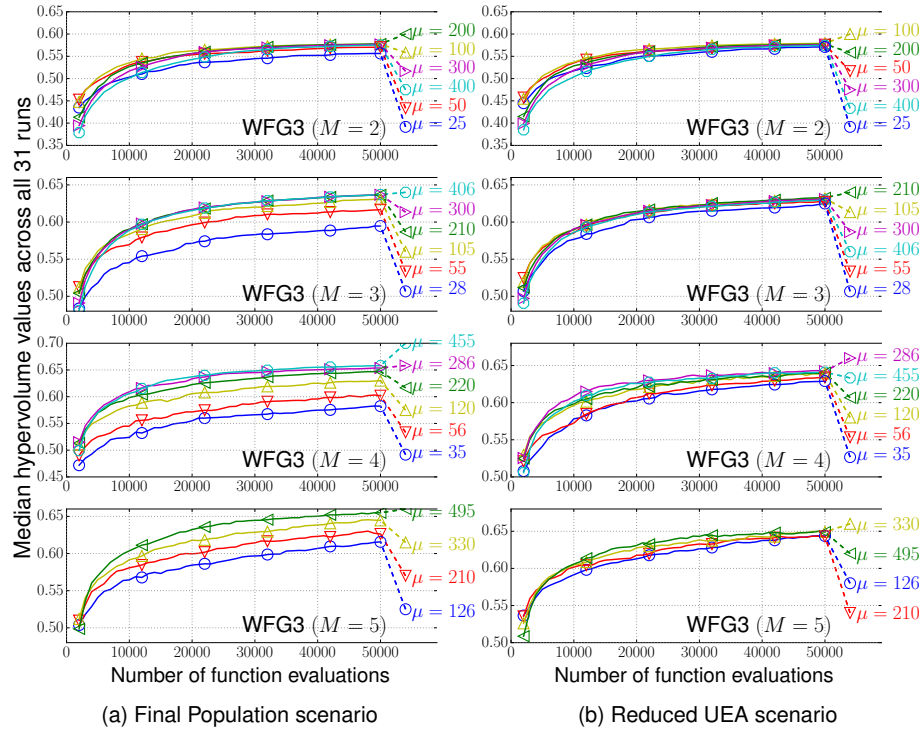


Figure S.7: Performance of MOEA/D with various  $\mu$  settings on the WFG3 problem with  $M \in \{2, 3, 4, 5\}$ . The horizontal and vertical axes represent the number of function evaluations and the HV values, respectively.



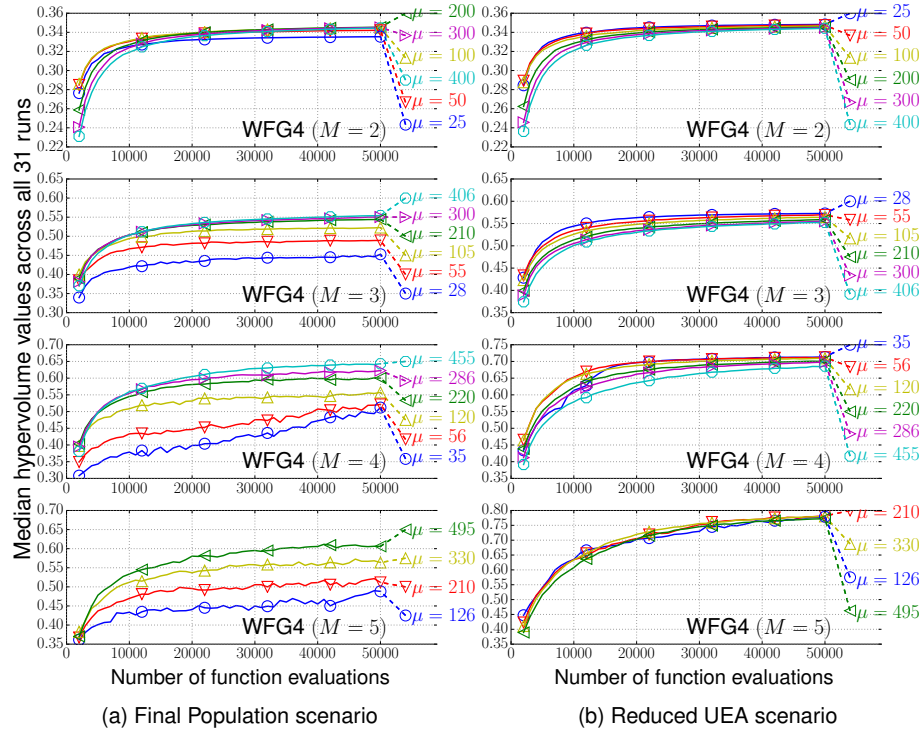


Figure S.8: Performance of MOEA/D with various  $\mu$  settings on the WFG4 problem with  $M \in \{2, 3, 4, 5\}$ . The horizontal and vertical axes represent the number of function evaluations and the HV values, respectively.

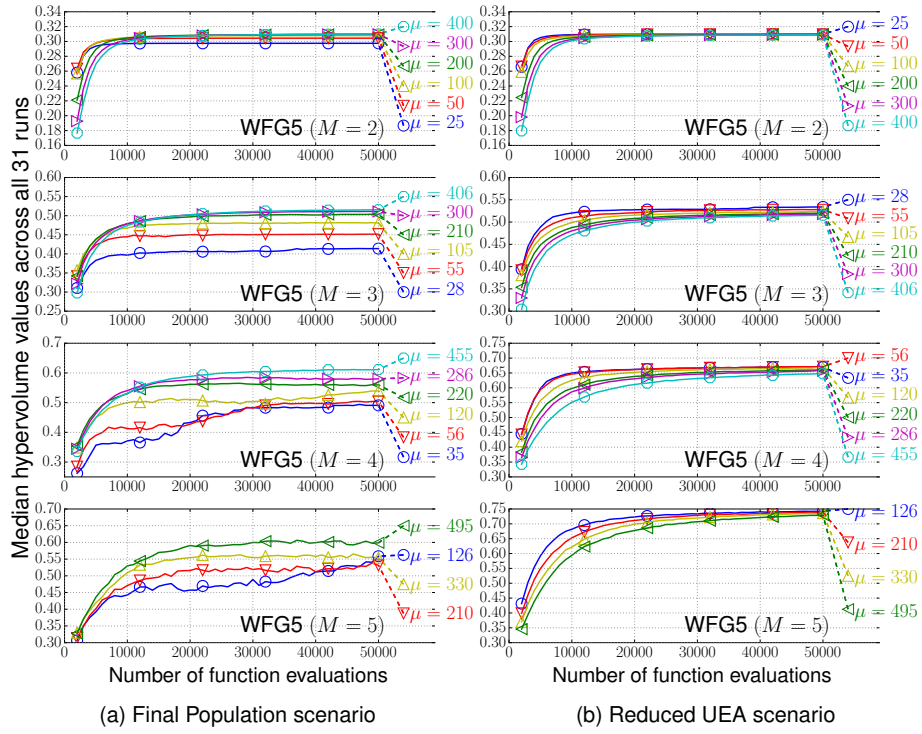


Figure S.9: Performance of MOEA/D with various  $\mu$  settings on the WFG5 problem with  $M \in \{2, 3, 4, 5\}$ . The horizontal and vertical axes represent the number of function evaluations and the HV values, respectively.

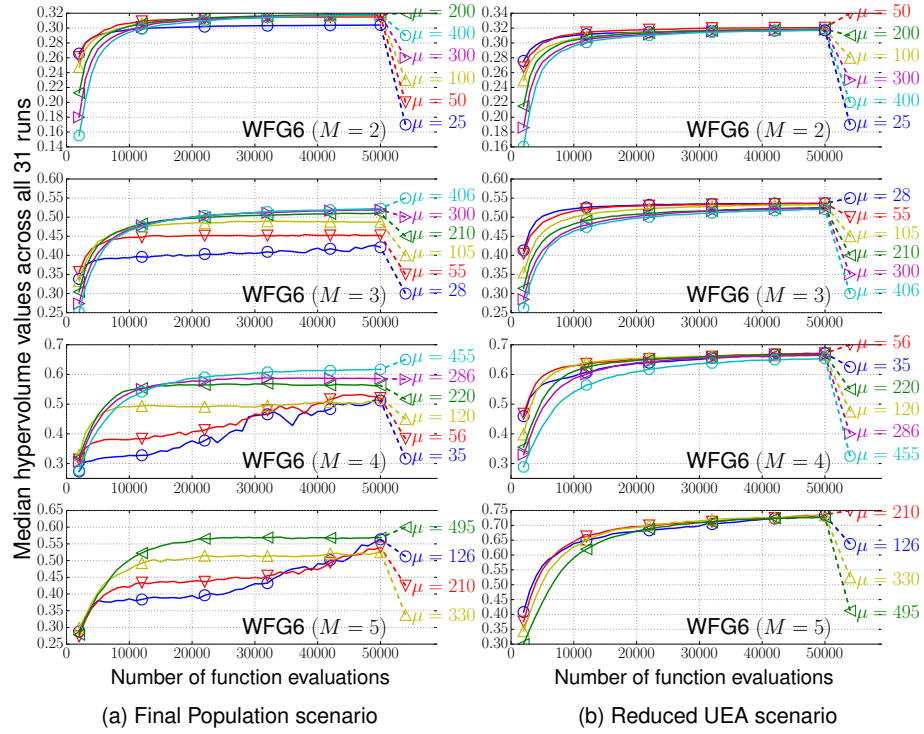


Figure S.10: Performance of MOEA/D with various  $\mu$  settings on the WFG6 problem with  $M \in \{2, 3, 4, 5\}$ . The horizontal and vertical axes represent the number of function evaluations and the HV values, respectively.

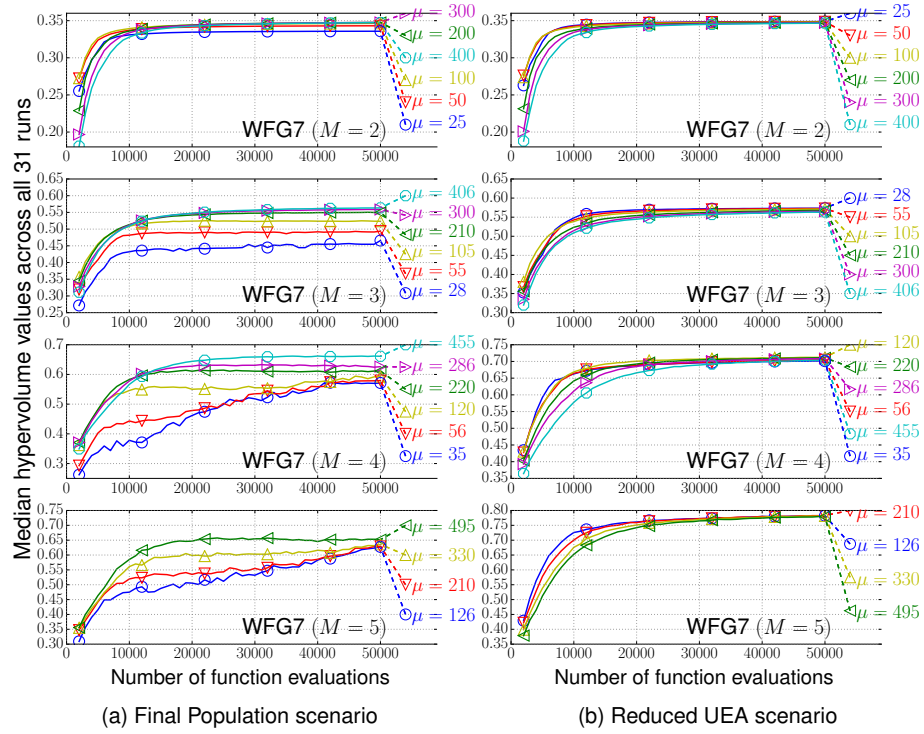


Figure S.11: Performance of MOEA/D with various  $\mu$  settings on the WFG7 problem with  $M \in \{2, 3, 4, 5\}$ . The horizontal and vertical axes represent the number of function evaluations and the HV values, respectively.

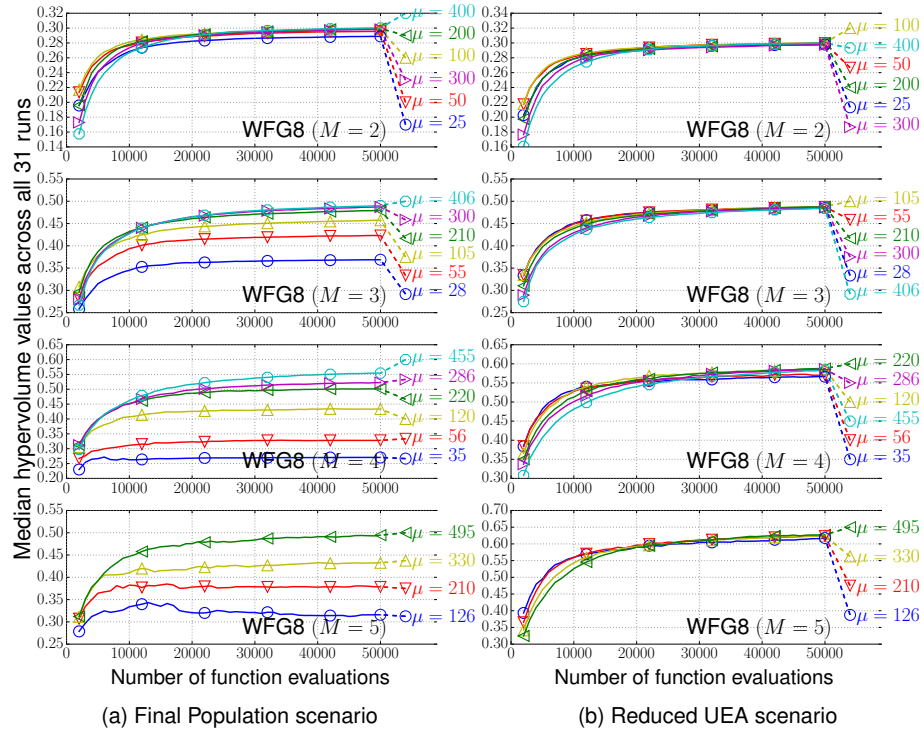


Figure S.12: Performance of MOEA/D with various  $\mu$  settings on the WFG8 problem with  $M \in \{2, 3, 4, 5\}$ . The horizontal and vertical axes represent the number of function evaluations and the HV values, respectively.

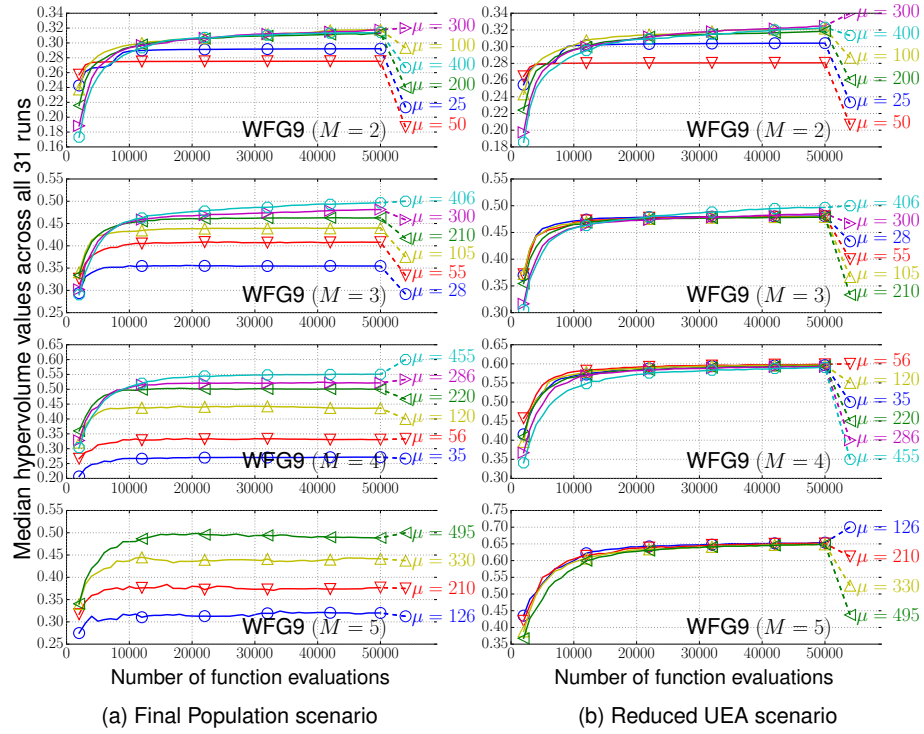


Figure S.13: Performance of MOEA/D with various  $\mu$  settings on the WFG9 problem with  $M \in \{2, 3, 4, 5\}$ . The horizontal and vertical axes represent the number of function evaluations and the HV values, respectively.

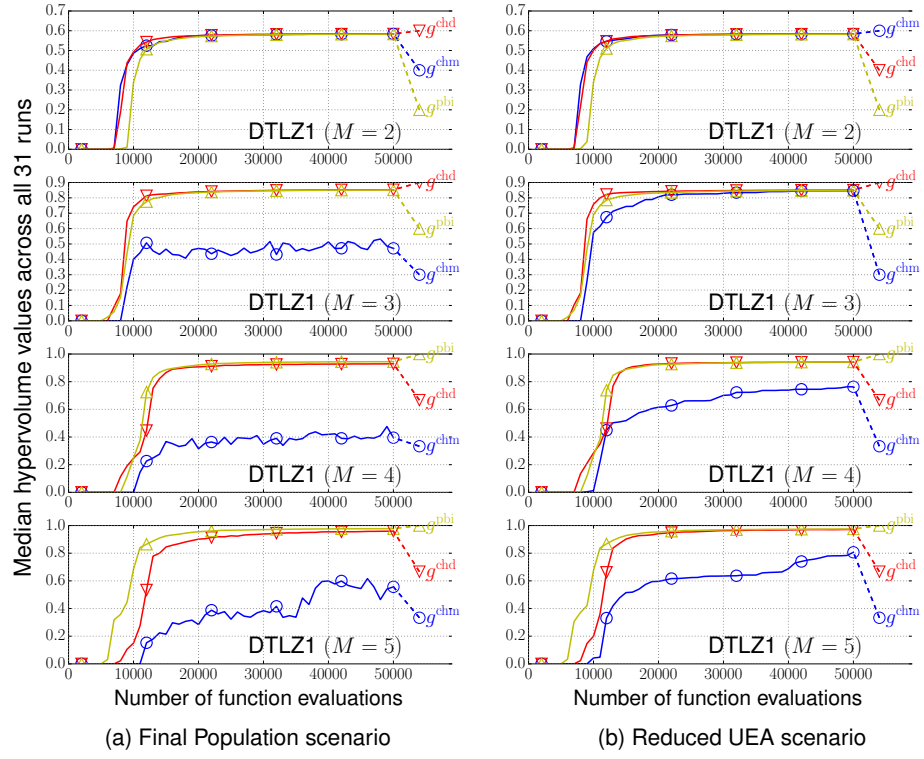


Figure S.14: Performance of MOEA/D with the three scalarizing functions ( $g^{\text{chm}}$ ,  $g^{\text{chd}}$ , and  $g^{\text{pbi}}$  with  $\theta = 5$ ) on the DTLZ1 problem with  $M \in \{2, 3, 4, 5\}$ . The horizontal and vertical axes represent the number of function evaluations and the HV values, respectively.

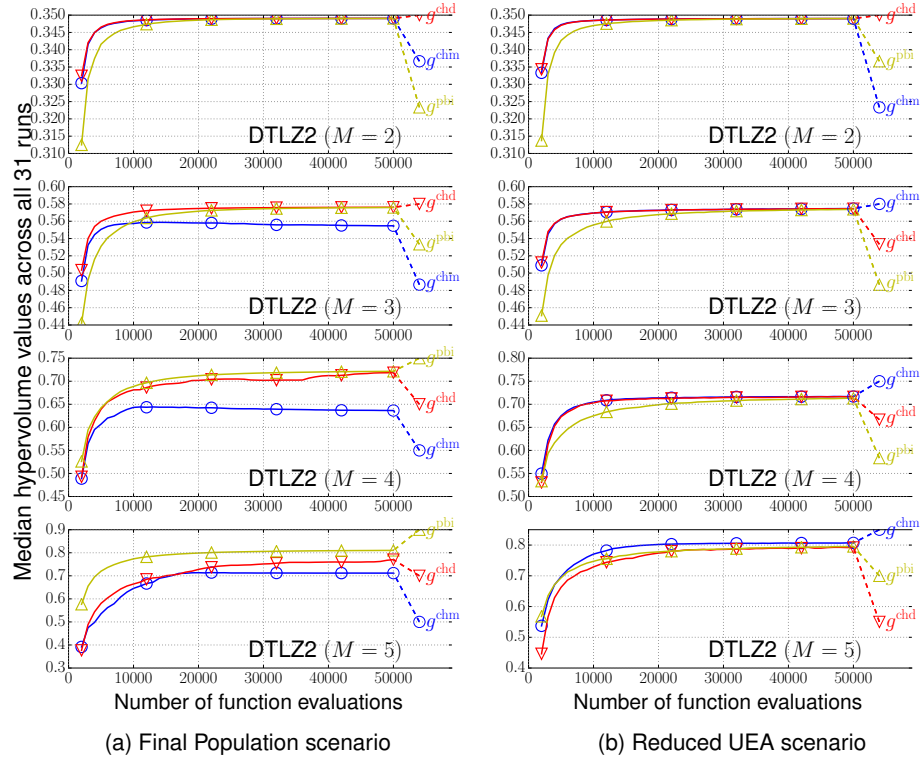


Figure S.15: Performance of MOEA/D with the three scalarizing functions ( $g^{\text{chm}}$ ,  $g^{\text{chd}}$ , and  $g^{\text{pbi}}$  with  $\theta = 5$ ) on the DTLZ2 problem with  $M \in \{2, 3, 4, 5\}$ . The horizontal and vertical axes represent the number of function evaluations and the HV values, respectively.



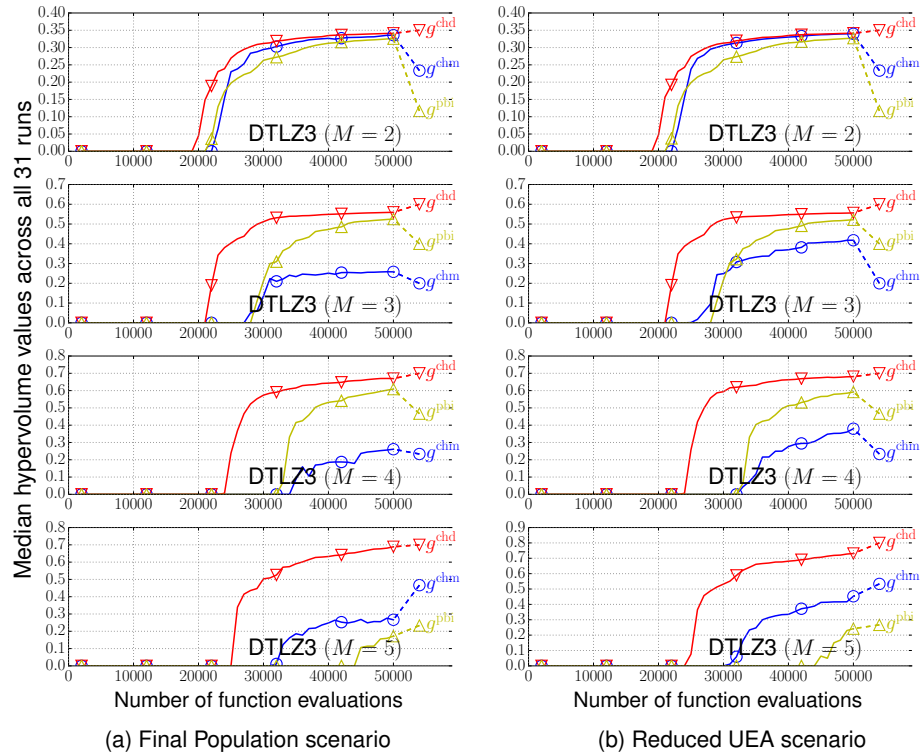


Figure S.16: Performance of MOEA/D with the three scalarizing functions ( $g^{\text{chm}}$ ,  $g^{\text{chd}}$ , and  $g^{\text{pbi}}$  with  $\theta = 5$ ) on the DTLZ3 problem with  $M \in \{2, 3, 4, 5\}$ . The horizontal and vertical axes represent the number of function evaluations and the HV values, respectively.

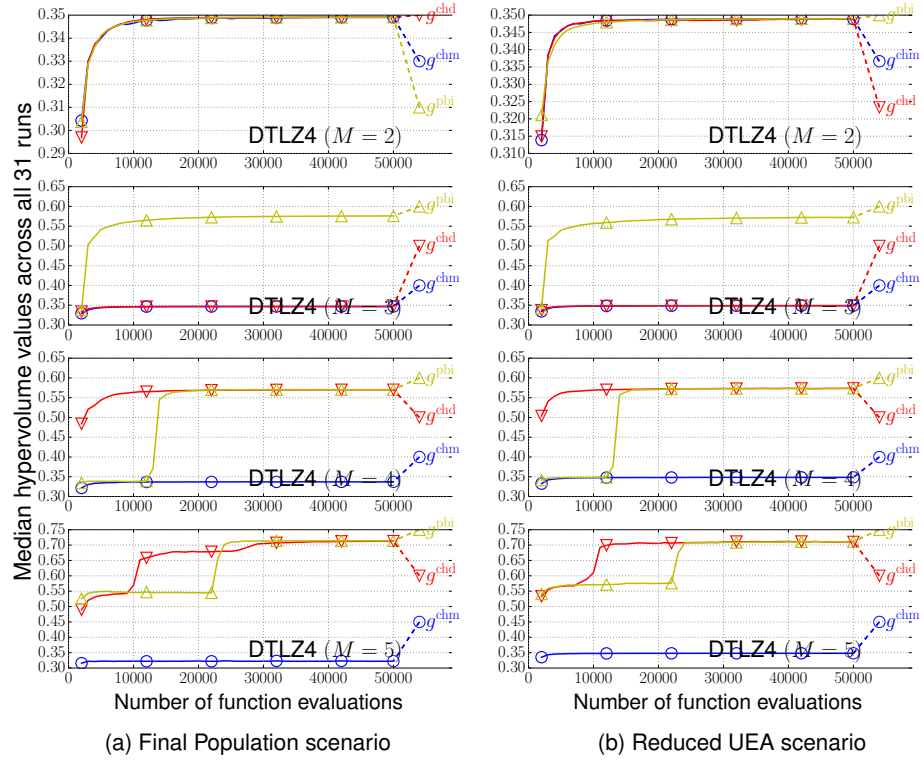


Figure S.17: Performance of MOEA/D with the three scalarizing functions ( $g^{\text{chm}}$ ,  $g^{\text{chd}}$ , and  $g^{\text{pbi}}$  with  $\theta = 5$ ) on the DTLZ4 problem with  $M \in \{2, 3, 4, 5\}$ . The horizontal and vertical axes represent the number of function evaluations and the HV values, respectively.

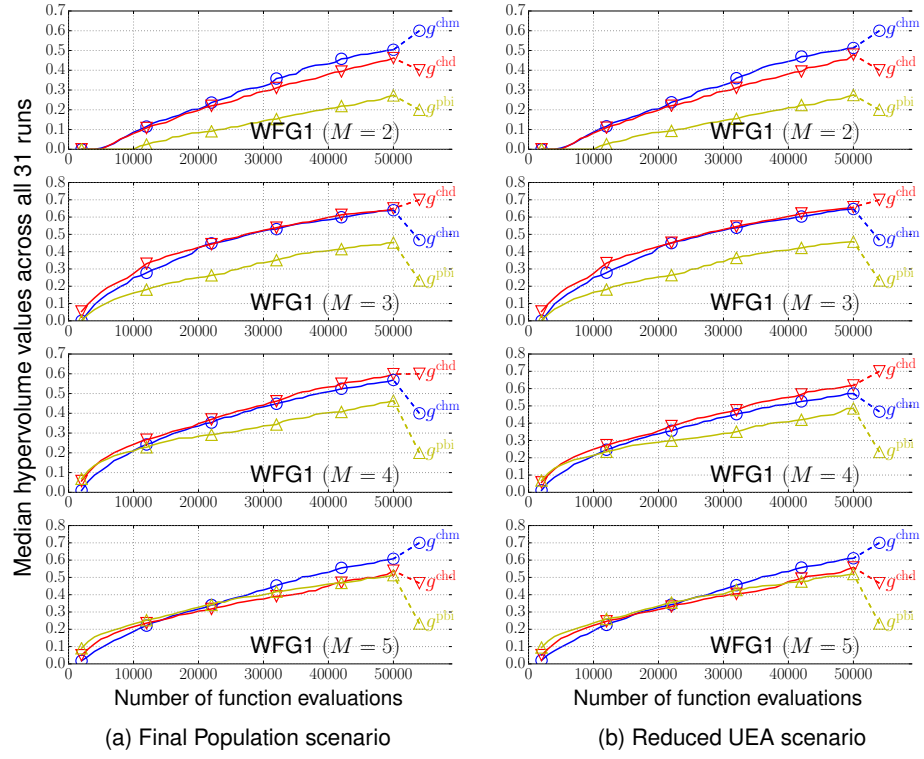


Figure S.18: Performance of MOEA/D with the three scalarizing functions ( $g^{\text{chm}}$ ,  $g^{\text{chd}}$ , and  $g^{\text{pbi}}$  with  $\theta = 5$ ) on the WFG1 problem with  $M \in \{2, 3, 4, 5\}$ . The horizontal and vertical axes represent the number of function evaluations and the HV values, respectively.

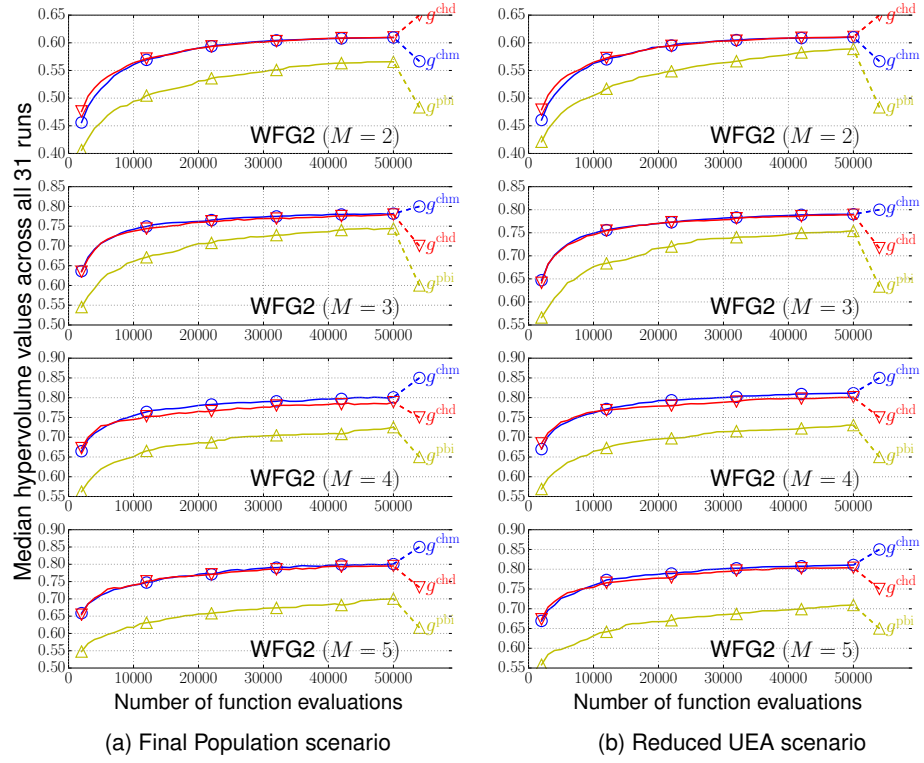


Figure S.19: Performance of MOEA/D with the three scalarizing functions ( $g^{\text{chm}}$ ,  $g^{\text{chd}}$ , and  $g^{\text{pbi}}$  with  $\theta = 5$ ) on the WFG2 problem with  $M \in \{2, 3, 4, 5\}$ . The horizontal and vertical axes represent the number of function evaluations and the HV values, respectively.

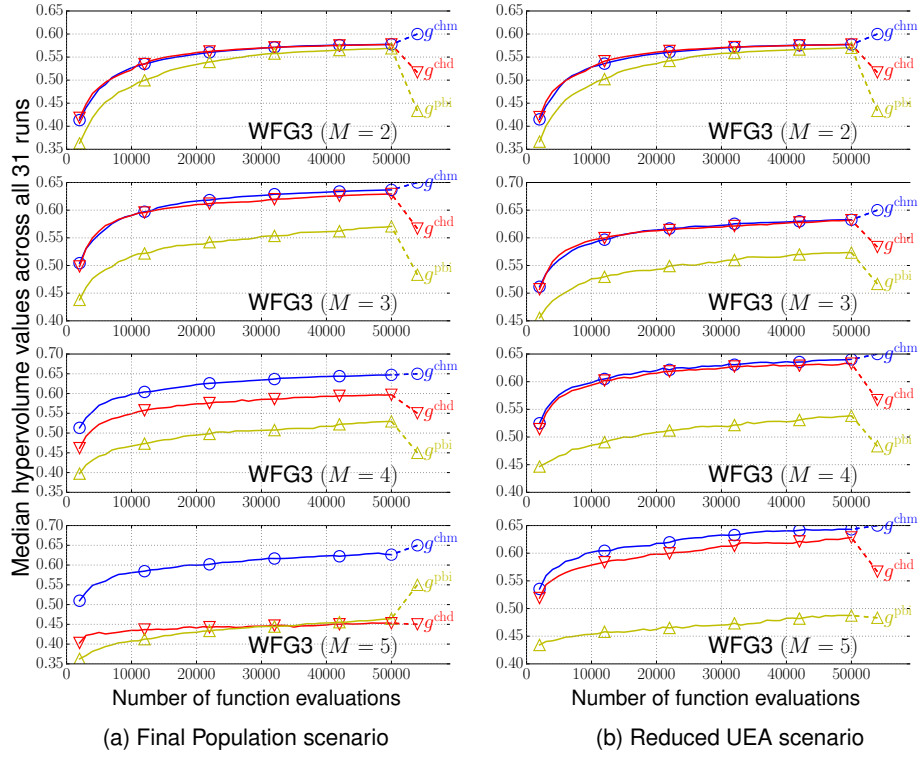


Figure S.20: Performance of MOEA/D with the three scalarizing functions ( $g^{\text{chm}}$ ,  $g^{\text{chd}}$ , and  $g^{\text{phi}}$  with  $\theta = 5$ ) on the WFG3 problem with  $M \in \{2, 3, 4, 5\}$ . The horizontal and vertical axes represent the number of function evaluations and the HV values, respectively.

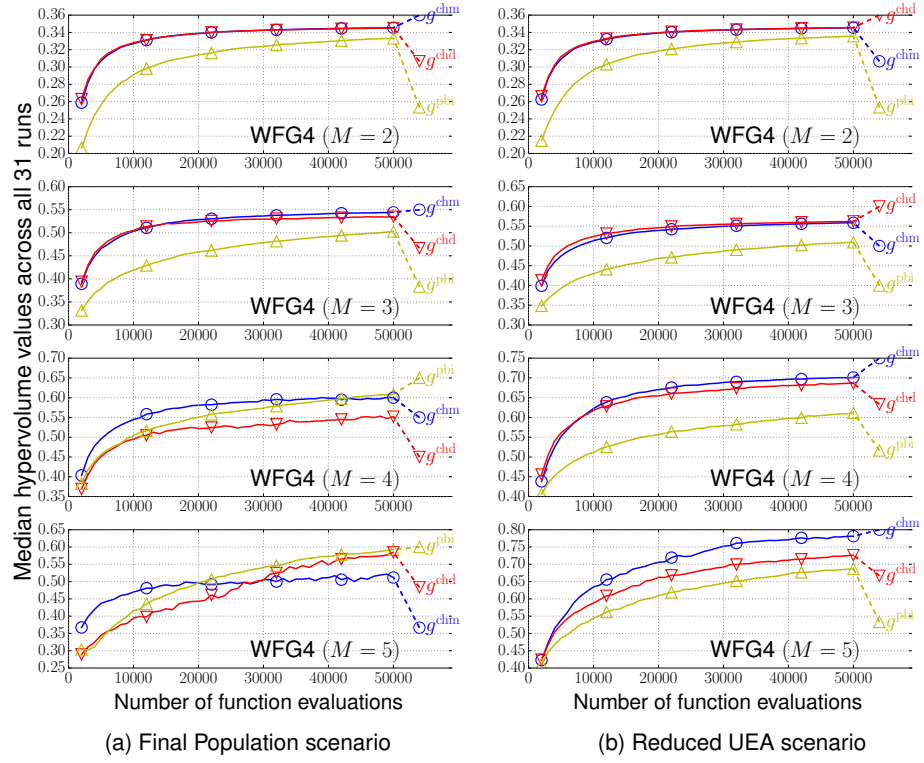


Figure S.21: Performance of MOEA/D with the three scalarizing functions ( $g^{\text{chm}}$ ,  $g^{\text{chd}}$ , and  $g^{\text{pbi}}$  with  $\theta = 5$ ) on the WFG4 problem with  $M \in \{2, 3, 4, 5\}$ . The horizontal and vertical axes represent the number of function evaluations and the HV values, respectively.

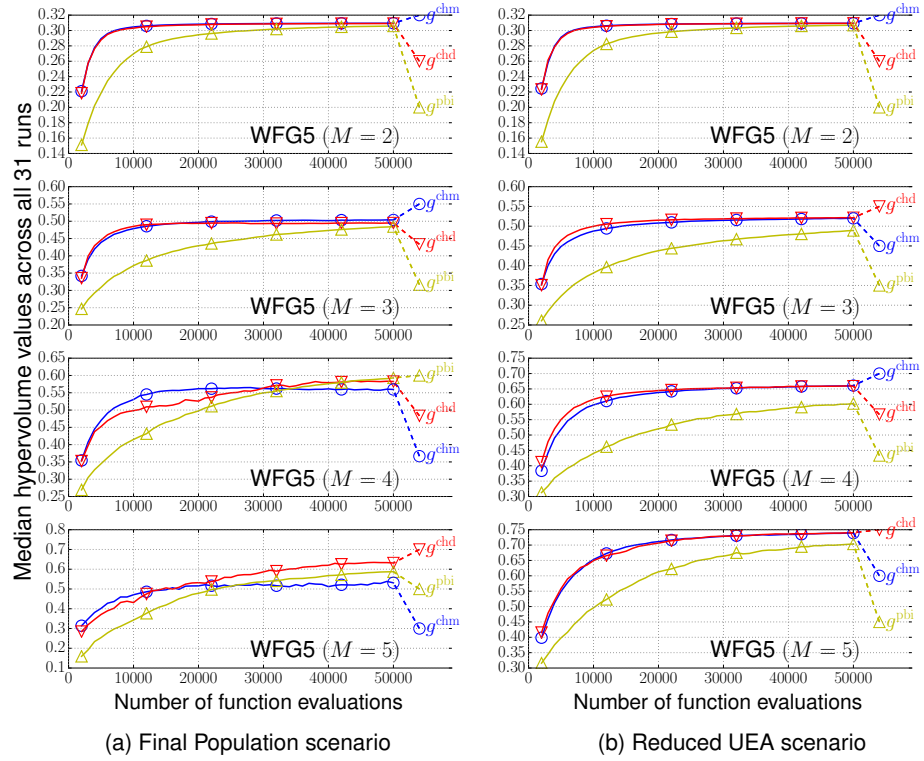


Figure S.22: Performance of MOEA/D with the three scalarizing functions ( $g^{\text{chm}}$ ,  $g^{\text{chd}}$ , and  $g^{\text{pbi}}$  with  $\theta = 5$ ) on the WFG5 problem with  $M \in \{2, 3, 4, 5\}$ . The horizontal and vertical axes represent the number of function evaluations and the HV values, respectively.

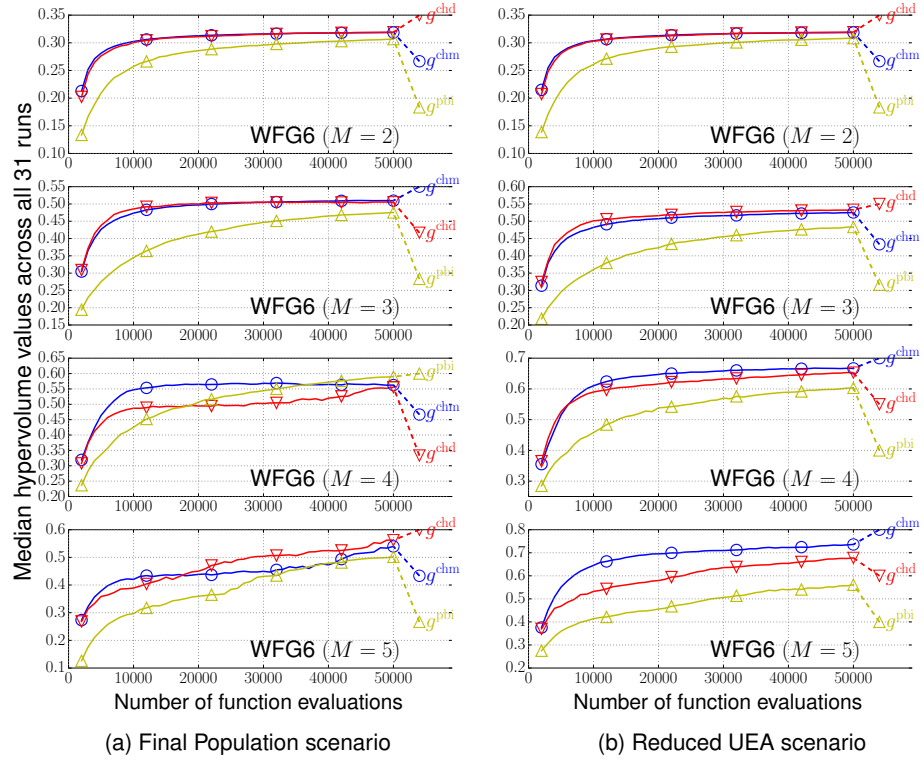


Figure S.23: Performance of MOEA/D with the three scalarizing functions ( $g^{\text{chm}}$ ,  $g^{\text{chd}}$ , and  $g^{\text{phi}}$  with  $\theta = 5$ ) on the WFG6 problem with  $M \in \{2, 3, 4, 5\}$ . The horizontal and vertical axes represent the number of function evaluations and the HV values, respectively.



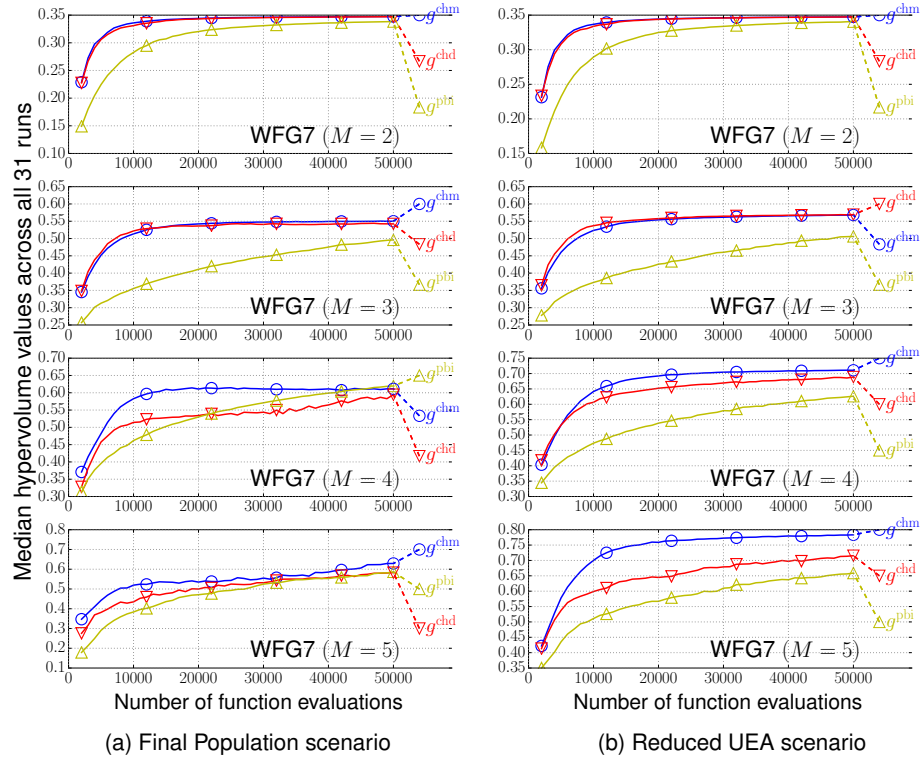


Figure S.24: Performance of MOEA/D with the three scalarizing functions ( $g^{\text{chm}}$ ,  $g^{\text{chd}}$ , and  $g^{\text{pbi}}$  with  $\theta = 5$ ) on the WFG7 problem with  $M \in \{2, 3, 4, 5\}$ . The horizontal and vertical axes represent the number of function evaluations and the HV values, respectively.

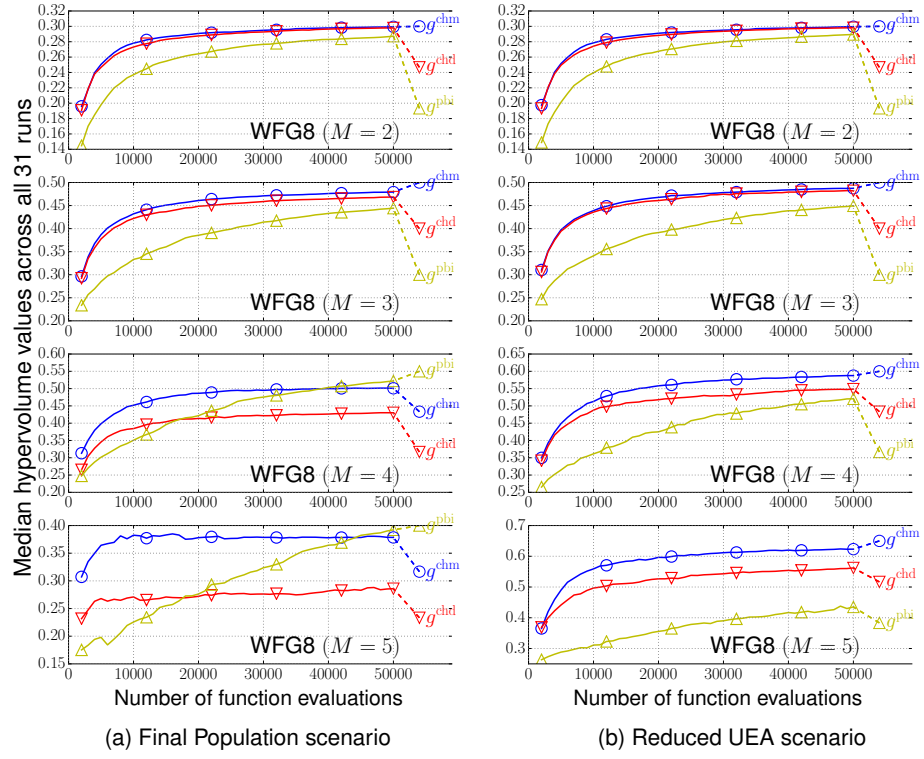


Figure S.25: Performance of MOEA/D with the three scalarizing functions ( $g^{\text{chm}}$ ,  $g^{\text{chd}}$ , and  $g^{\text{pbi}}$  with  $\theta = 5$ ) on the WFG8 problem with  $M \in \{2, 3, 4, 5\}$ . The horizontal and vertical axes represent the number of function evaluations and the HV values, respectively.

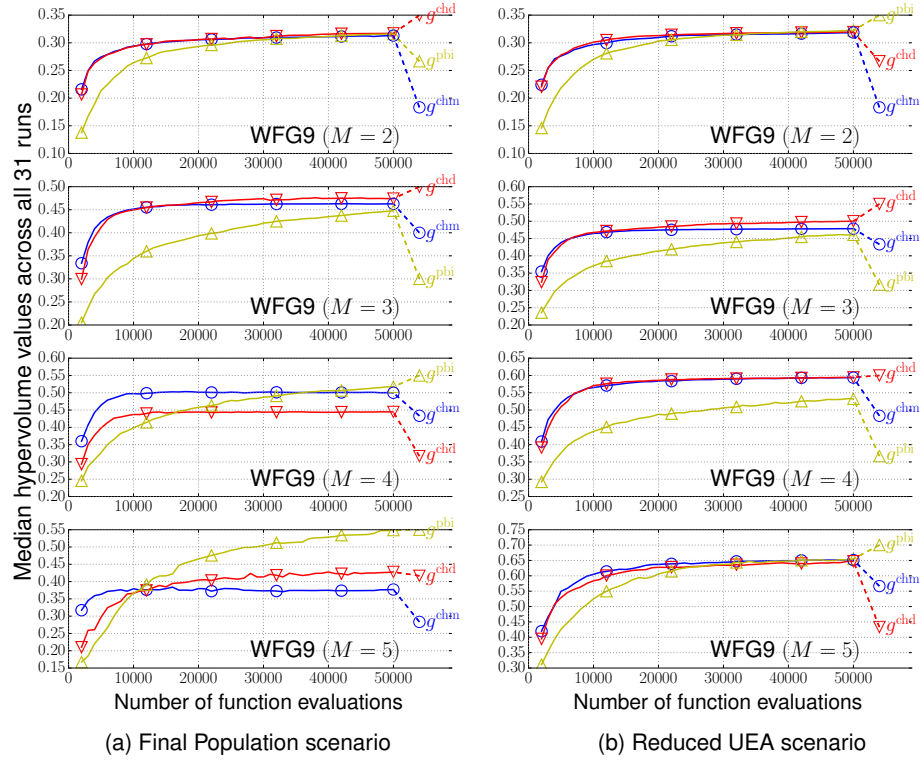


Figure S.26: Performance of MOEA/D with the three scalarizing functions ( $g^{\text{chm}}$ ,  $g^{\text{chd}}$ , and  $g^{\text{pbi}}$  with  $\theta = 5$ ) on the WFG9 problem with  $M \in \{2, 3, 4, 5\}$ . The horizontal and vertical axes represent the number of function evaluations and the HV values, respectively.

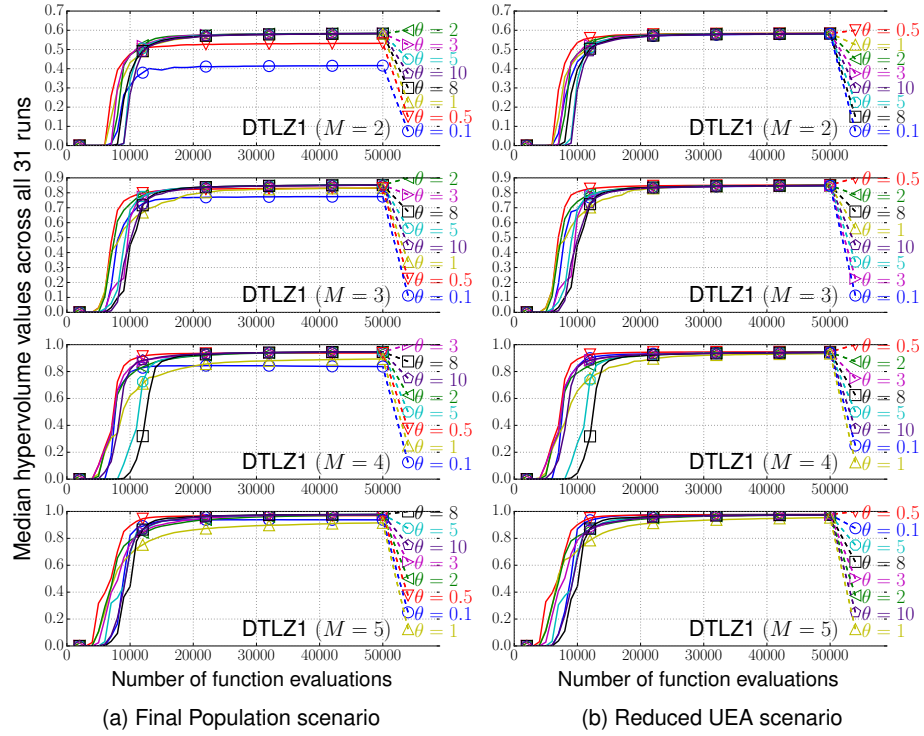


Figure S.27: Performance of MOEA/D using the PBI function  $g^{\text{Pbi}}$  with various  $\theta$  values on the DTLZ1 problem with  $M \in \{2, 3, 4, 5\}$ . The horizontal and vertical axes represent the number of function evaluations and the HV values, respectively.

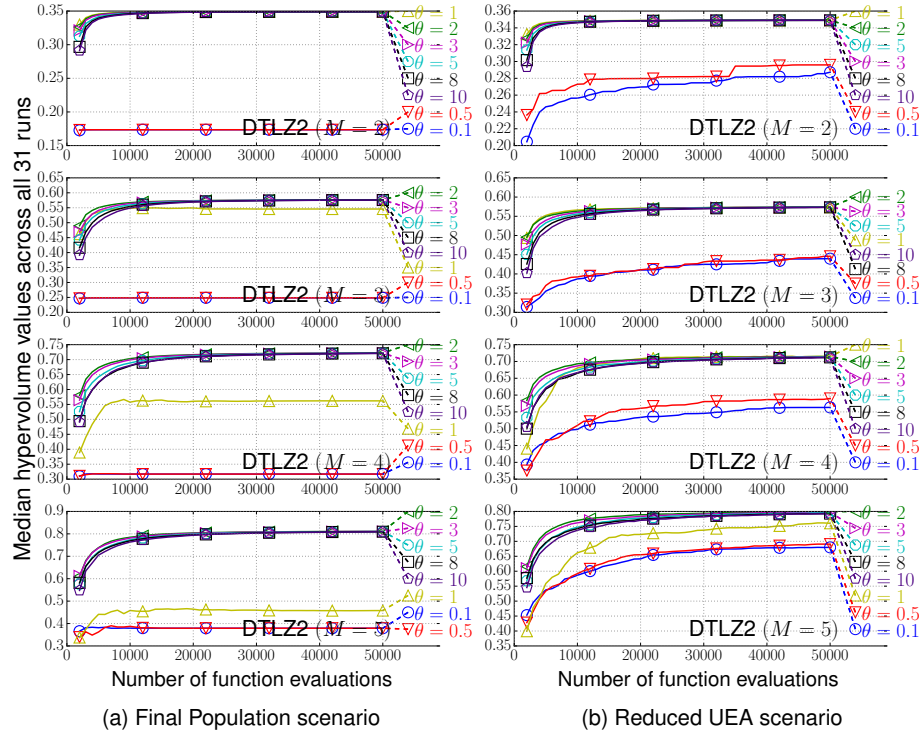


Figure S.28: Performance of MOEA/D using the PBI function  $g^{\text{Pbi}}$  with various  $\theta$  values on the DTLZ2 problem with  $M \in \{2, 3, 4, 5\}$ . The horizontal and vertical axes represent the number of function evaluations and the HV values, respectively.



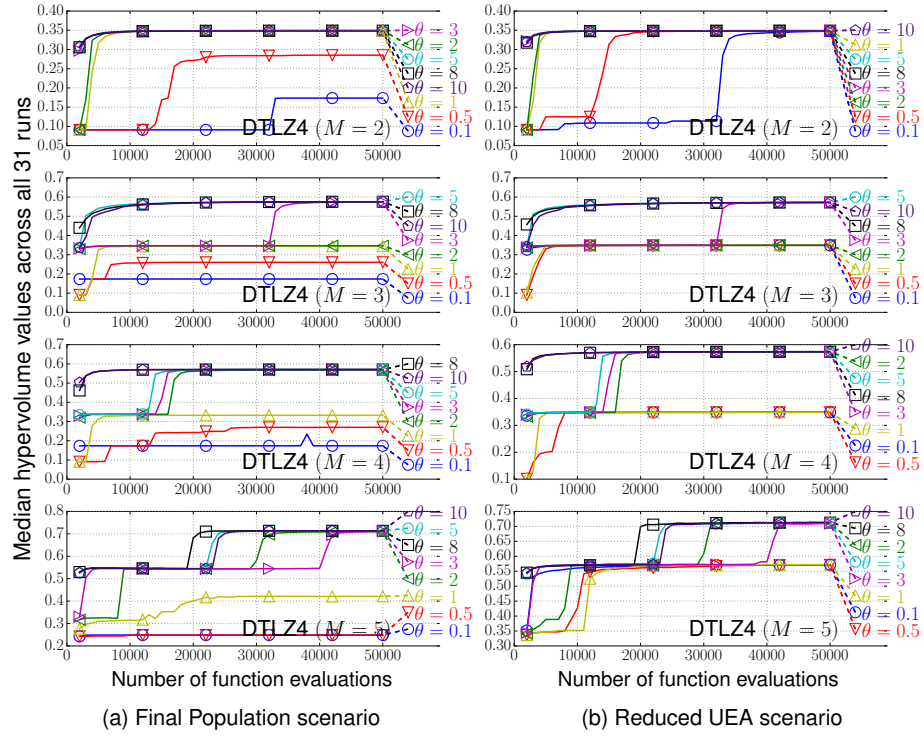


Figure S.30: Performance of MOEA/D using the PBI function  $g^{\text{Pbi}}$  with various  $\theta$  values on the DTLZ4 problem with  $M \in \{2, 3, 4, 5\}$ . The horizontal and vertical axes represent the number of function evaluations and the HV values, respectively.

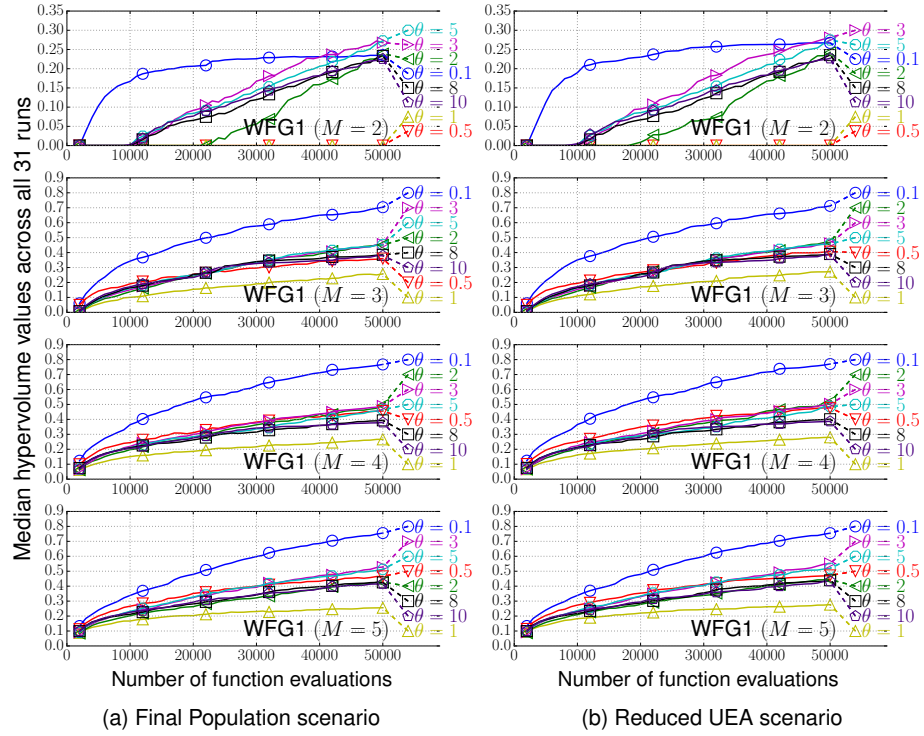


Figure S.31: Performance of MOEA/D using the PBI function  $g^{\text{pbi}}$  with various  $\theta$  values on the WFG1 problem with  $M \in \{2, 3, 4, 5\}$ . The horizontal and vertical axes represent the number of function evaluations and the HV values, respectively.



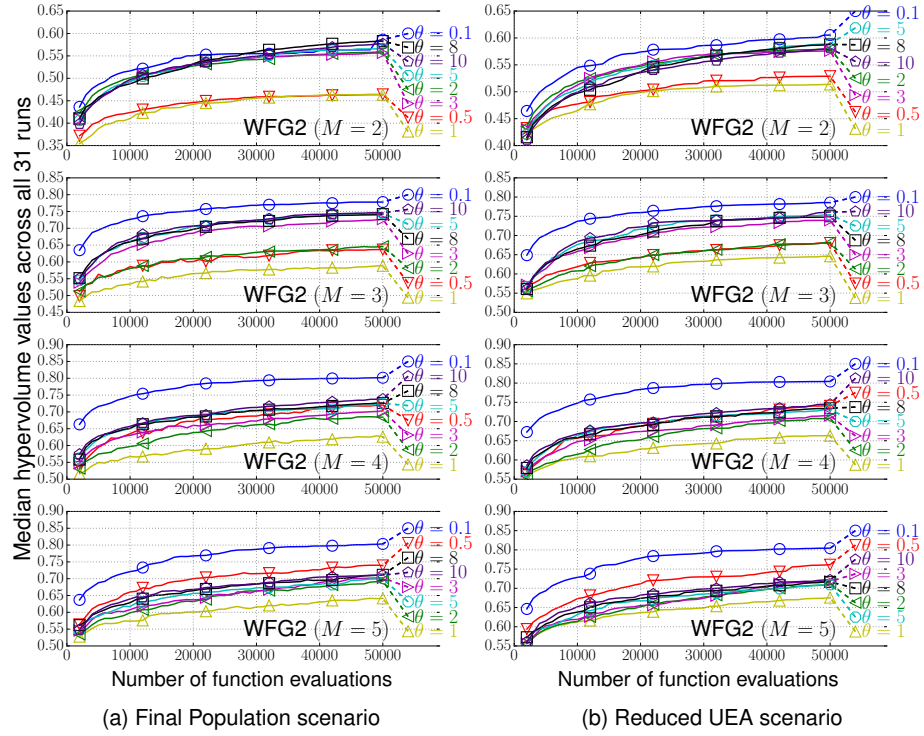


Figure S.32: Performance of MOEA/D using the PBI function  $g^{\text{pbi}}$  with various  $\theta$  values on the WFG2 problem with  $M \in \{2, 3, 4, 5\}$ . The horizontal and vertical axes represent the number of function evaluations and the HV values, respectively.

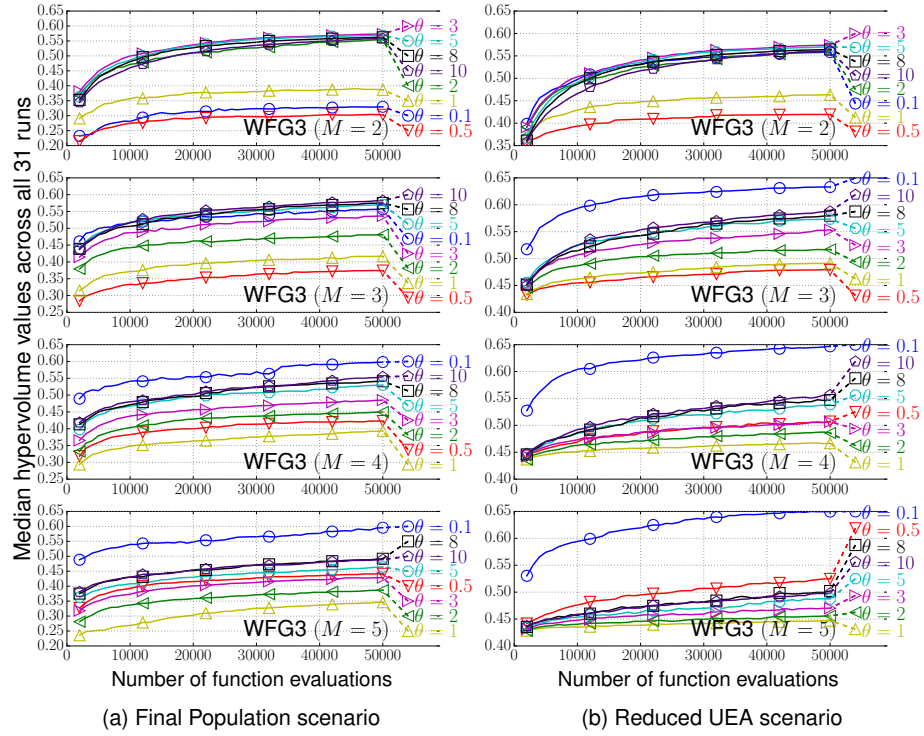


Figure S.33: Performance of MOEA/D using the PBI function  $g^{\text{pbi}}$  with various  $\theta$  values on the WFG3 problem with  $M \in \{2, 3, 4, 5\}$ . The horizontal and vertical axes represent the number of function evaluations and the HV values, respectively.

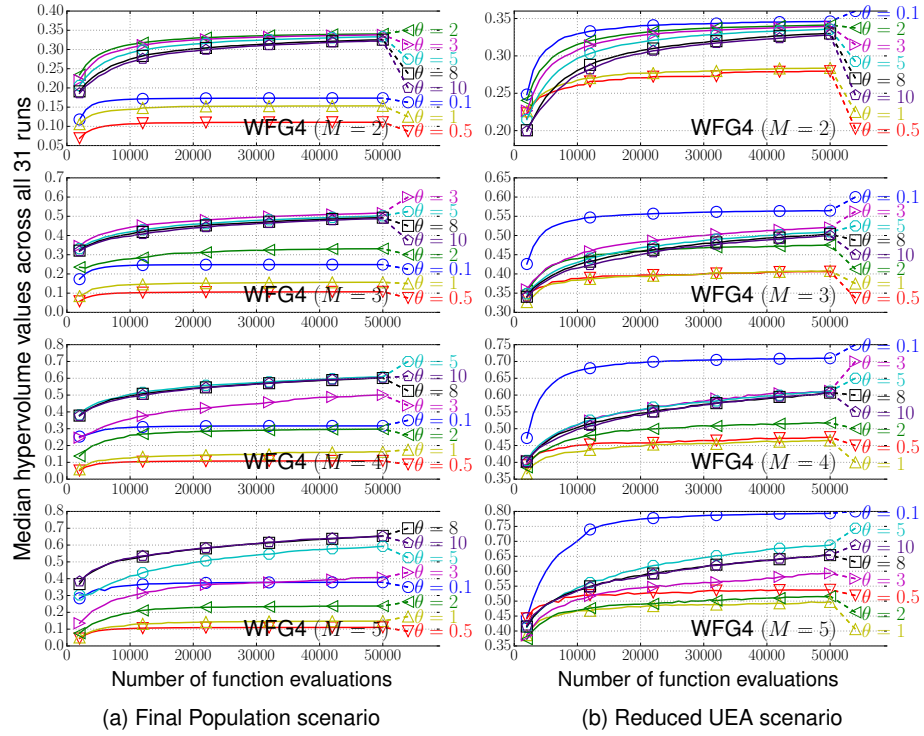


Figure S.34: Performance of MOEA/D using the PBI function  $g^{\text{pbi}}$  with various  $\theta$  values on the WFG4 problem with  $M \in \{2, 3, 4, 5\}$ . The horizontal and vertical axes represent the number of function evaluations and the HV values, respectively.

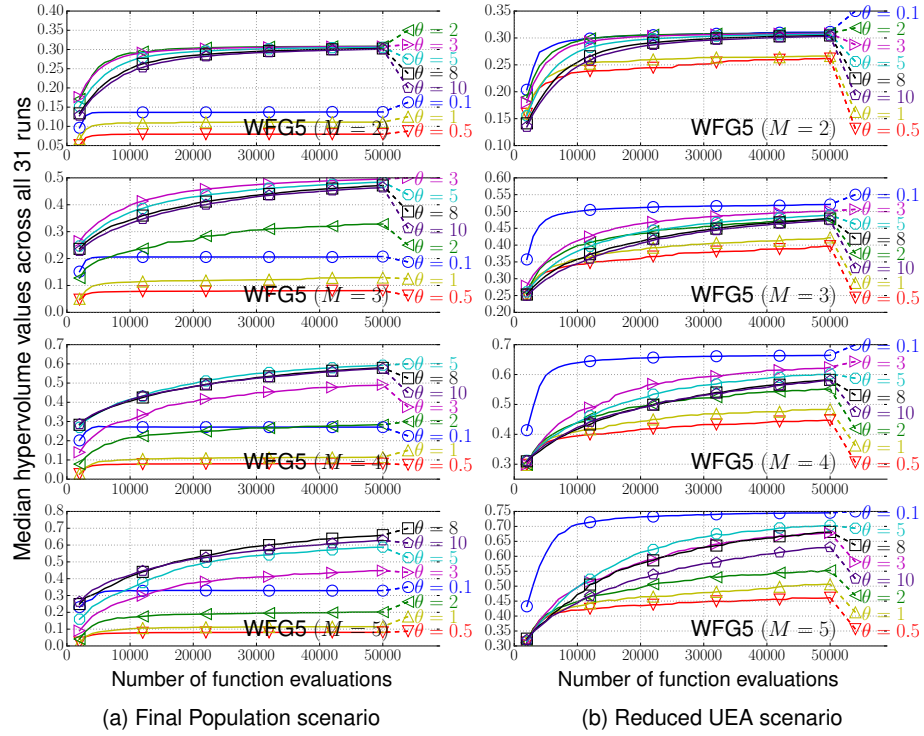


Figure S.35: Performance of MOEA/D using the PBI function  $g^{\text{pbi}}$  with various  $\theta$  values on the WFG5 problem with  $M \in \{2, 3, 4, 5\}$ . The horizontal and vertical axes represent the number of function evaluations and the HV values, respectively.



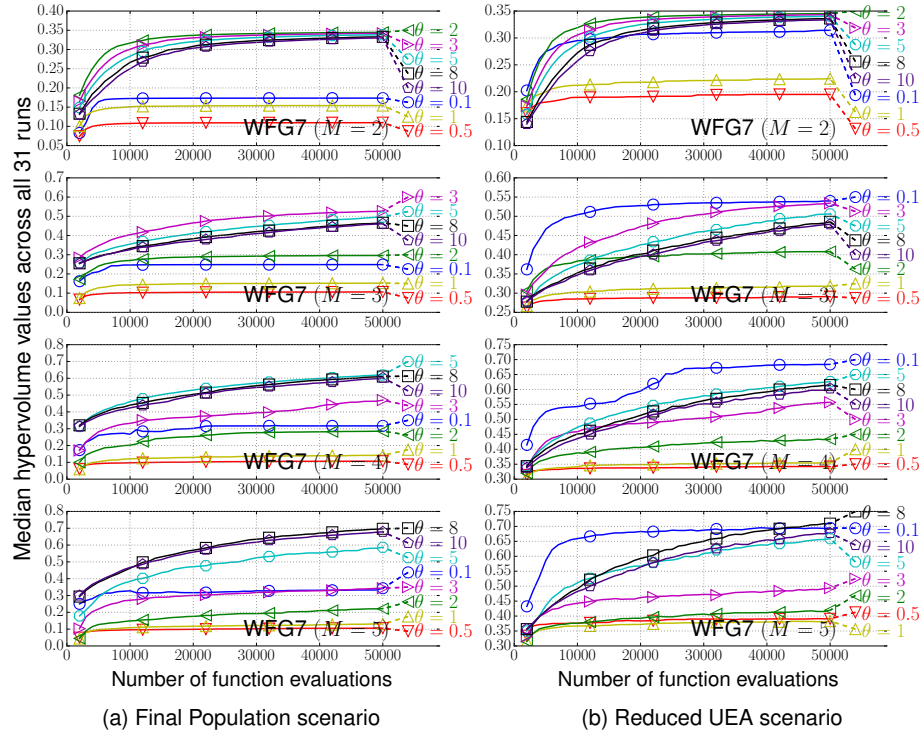


Figure S.37: Performance of MOEA/D using the PBI function  $g^{\text{pbi}}$  with various  $\theta$  values on the WFG7 problem with  $M \in \{2, 3, 4, 5\}$ . The horizontal and vertical axes represent the number of function evaluations and the HV values, respectively.

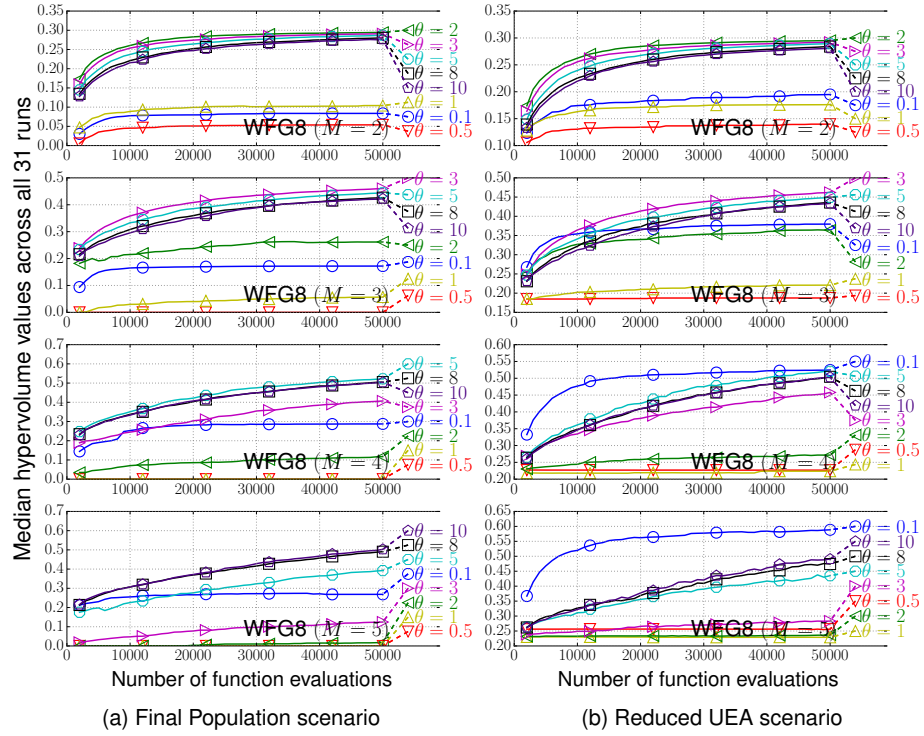


Figure S.38: Performance of MOEA/D using the PBI function  $g^{\text{pbi}}$  with various  $\theta$  values on the WFG8 problem with  $M \in \{2, 3, 4, 5\}$ . The horizontal and vertical axes represent the number of function evaluations and the HV values, respectively.

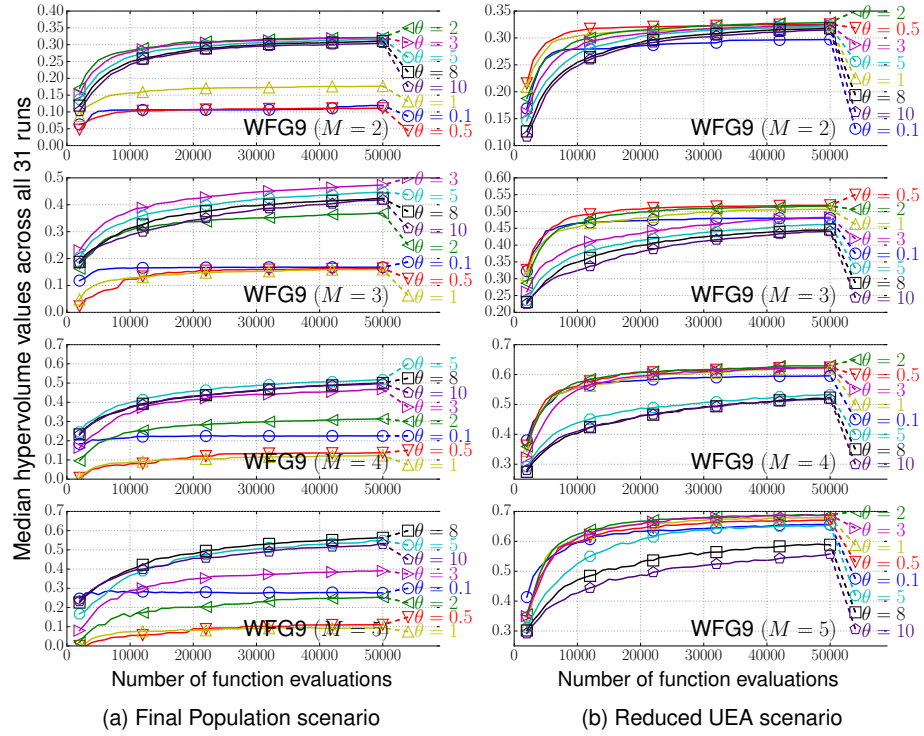


Figure S.39: Performance of MOEA/D using the PBI function  $g^{\text{pbi}}$  with various  $\theta$  values on the WFG9 problem with  $M \in \{2, 3, 4, 5\}$ . The horizontal and vertical axes represent the number of function evaluations and the HV values, respectively.